A New Surface Integral Formulation For Wideband Impedance Extraction of 3-D Structures *

Ben Song †, Zhenhai Zhu †, John D. Rockway *, Jacob White †

† Department of Electrical Engineering and Computer Science
Massachusetts Institute of Technology, Cambridge, MA 02139
{bsong01, zhzhu, white}@mit.edu
* Lawrence Livemore National Laboratory, Berkeley, CA 27599
jdrockway@llnl.gov

Abstract

Detailed electromagnetic analysis of three-dimensional structures in multi-layered dielectric media is critical for automatic generation of equivalent circuit models for the interconnects and packages in RF or mixed signal integrated circuits. In this paper we present a new wideband surface integral formulation that can be readily combined with the well-established layered Green's function techniques. In discretizing the formulation, we have used the well-known RWG linear basis function to reduce the number of unknowns. Using a so-called loop-star basis transformation and the frequency normalization, the accuracy at low frequencies has been improved substantially. Several numerical examples are used to validate the accuracy and robustness of this new formulation.

1. Introduction

RF and mixed-signal systems are extremely sensitive to high-frequency electromagnetic coupling effects associated with the interconnect, but accurately determining those effects often requires analyzing hundreds of simultaneously interacting conductors. Accelerated integral equation based methods have demonstrated an ability to perform detailed electromagnetic analysis of complicated 3-D structures [1, 2, 3, 4], and efforts continue to improve computational efficiency by reducing the number of discretization unknowns. For example, frequency dependent global basis functions have been used to reduce the number of unknowns in volume integral equation methods [5], and surface integral formulations have been employed to avoid generating frequency-dependent discretizations of conductor and substrate interiors [6, 7, 8].

One of the persistent challenges in developing methods based on surface integral formulations is finding an approach that is truly wideband, and there has been much recent progress. One example is a surface integral formulation described in [6, 9], which was combined with the pre-corrected FFT acceleration algorithm to produce the program FastImp [10, 11]. Although FastImp is a useful tool, the surface integral formulation on which the program is based has two problems that limit the program's generality. First, the integral formulation was derived from scalar Helmholtz equations and uses $\vec{E}$ and $\frac{\partial \vec{E}}{\partial n}$ as its unknowns. This makes it very difficult to use the well-established multilayered media Green's functions [12, 13] for the analysis of 3D structures embedded into multi-layered dielectric media. Second, the formulation uses two different methods to calculate external port current at low frequencies and high frequencies. This inconsistency can cause continuity difficulties and interferes with using model order reduction [14].

To address the difficulties listed above, we developed a new surface integral formulation derived from vector Helmholtz wave equations, and describe the derivation in Section 2. As briefly described in Section 3, this approach generates a formulation for which it is immediately possible to use the well-established techniques for multilayered media, port current computation, and surface discretization. In section 4, results from numerical experiments are used to show that the new formulation is accurate and robust across wide frequency range. Conclusions are given in Section 5.

2. Derivation of the Surface Integral Formulation

For the following derivation, assume the 3D structure consists of N conductors, denoted as $V_i, i = 1,2,\cdots,N$ and let the free space be denoted as V_0.

2.1 Governing equations

In free space, the independent Maxwell's equations in time-harmonic form are [15]

$$\nabla \times \vec{E} = -j\omega\mu_0\vec{H} \quad (1)$$

$$\nabla \times \vec{H} = \vec{J} + j\omega\varepsilon_0\vec{E} \quad (2)$$

$$\nabla \cdot \vec{J} = -j\omega\rho \quad (3)$$

where $\vec{E}$,$\vec{H}$,$\vec{J}$,ρ,μ_0 and ε_0 denote the electric field, magnetic field, current density, charge density, permeability and permittivity, respectively. The constitutive equation for the current density $\vec{J}$ inside each conductor is

$$\vec{J}(\vec{r}) = \sigma_i\vec{E}(\vec{r}),\ \vec{r} \in V_i, \quad (4)$$

where σ_i is the conductivity of the i-th conductor. Equations (1) and (2) imply

$$\nabla \times \nabla \times \vec{E} - \omega^2\varepsilon_0\mu_0\vec{E} = -j\omega\mu_0\vec{J}. \quad (5)$$

And equations (1), (2) and (4) imply

$$\nabla \times \nabla \times \vec{H} - (\omega^2\varepsilon_0\mu_0 - j\omega\mu_0\sigma_i)\vec{H} = 0. \quad (6)$$

Since $\sigma_i \gg \omega\varepsilon_0$ for good conductors (such as copper and aluminum) up to the terahertz range [16], we could simplify equation (6) as

$$\nabla \times \nabla \times \vec{H} + j\omega\mu_0\sigma_i\vec{H} = 0. \quad (7)$$

Equations (5) and (7) are the governing equations inside each conductor V_i, and the equations (1- 3) are the governing equations in the surrounding free space V_0.

*This work was sponsored by the Semiconductor Research Corporation, the MARCO interconnect Focus Center, and the DARPA NeoCAD program managed by the Sensors Directorate of the Air Force Laboratory, USAF, Wright-Patterson AFB, and a grant from Intel.

ICCAD'03, November 11-13, 2003, San Jose, California, USA.

Proceedings of the International Conference on Computer Aided Design (ICCAD'03)
1092-3152/03 $ 17.00 © 2003 ACM

2.2 Surface integral representations

It is shown in [17] that the second vector Green's identity can be used to derive the surface integral representation for $\vec{E}$ field and $\vec{H}$ field from equations (5) and (7), respectively. The representation for $\vec{H}$ is

$$\begin{aligned} T(\vec{r})\vec{H}(\vec{r}) &= -\nabla\times\int_{S_i} dS(\vec{r}')G_1(\vec{r},\vec{r}')[\hat{n}\times\vec{H}](\vec{r}') \\ &+\nabla\int_{S_i} dS(\vec{r}')G_1(\vec{r},\vec{r}')[\hat{n}\cdot\vec{H}](\vec{r}') \\ &-(j\omega\varepsilon_0+\sigma_i)\int_{S_i} dS(\vec{r}')G_1(\vec{r},\vec{r}')[\hat{n}\times\vec{E}](\vec{r}'), \end{aligned} \tag{8}$$

where

$$G_1(\vec{r},\vec{r}') = \frac{e^{jk_1|\vec{r}-\vec{r}'|}}{4\pi|\vec{r}-\vec{r}'|},\ k_1=\sqrt{j\omega\mu_0\sigma_i}, \tag{9}$$

$$T(\vec{r}) = \begin{cases} 1 & \text{if } \vec{r}\in V_i \\ 1/2 & \text{if } \vec{r}\in S_i \\ 0 & \text{otherwise} \end{cases} \tag{10}$$

S_i is the surface of V_i. And the representation for $\vec{E}$ is

$$\begin{aligned} T(\vec{r})\vec{E}(\vec{r}) &= -\nabla\times\int_{S_i} dS(\vec{r}')G_0(\vec{r},\vec{r}')[\hat{n}\times\vec{E}](\vec{r}') \\ &+\nabla\int_{S_i} dS(\vec{r}')G_0(\vec{r},\vec{r}')[\hat{n}\cdot\vec{E}](\vec{r}') \\ &-(j\omega\mu_0)\int_{S_i} dS(\vec{r}')G_0(\vec{r},\vec{r}')[\hat{n}\times\vec{H}](\vec{r}') \\ &-(j\omega\mu_0)\int_{V_i} dV(\vec{r}')G_0(\vec{r},\vec{r}')\vec{J}(\vec{r}'), \end{aligned} \tag{11}$$

where

$$G_0(\vec{r},\vec{r}') = \frac{e^{jk_0|\vec{r}-\vec{r}'|}}{4\pi|\vec{r}-\vec{r}'|},\ k_0=\omega\sqrt{\varepsilon_0\mu_0}. \tag{12}$$

When $\vec{r}\in S_i$, the integrals in (8) and (11) should be the principle value integrals.

If we write equation (11) for each conductor separately but let $\vec{r}$ be fixed on the surface of a particular conductor V_k, and then sum up these equations, we obtain

$$\begin{aligned} \frac{1}{2}\vec{E}(\vec{r}) &= -\nabla\times\int_S dS(\vec{r}')G_0(\vec{r},\vec{r}')[\hat{n}\times\vec{E}](\vec{r}') \\ &+\nabla\int_S dS(\vec{r}')G_0(\vec{r},\vec{r}')[\hat{n}\cdot\vec{E}](\vec{r}') \\ &-(j\omega\mu_0)\int_S dS(\vec{r}')G_0(\vec{r},\vec{r}')[\hat{n}\times\vec{H}](\vec{r}') \\ &-(j\omega\mu_0)\int_V dV(\vec{r}')G_0(\vec{r},\vec{r}')\vec{J}(\vec{r}'), \end{aligned} \tag{13}$$

where $k=1,2,...,N$, S is the union of all conductor surfaces and V is the union of all conductor volumes.

All integrals in (8) and (13) except the last term in (13) are surface integrals. As pointed out in [10], we could use the well-known mixed potential integral equation (MPIE) to eliminate the undesirable volume integral term. The $\vec{E}$ field everywhere can be represented in terms of the scalar electric potential and the vector magnetic potential [18]

$$\begin{aligned} \vec{E}(\vec{r}) &= -j\omega\vec{A}(\vec{r})-\nabla\phi(\vec{r}) \\ &= -j\omega\mu_0\int_V dV(\vec{r}')G_0(\vec{r},\vec{r}')\vec{J}(\vec{r}')-\nabla\phi(\vec{r}) \end{aligned} \tag{14}$$

where

$$\phi(\vec{r}) = \int_S dS(\vec{r}')G_0(\vec{r},\vec{r}')\frac{\rho(\vec{r}')}{\varepsilon_0} \tag{15}$$

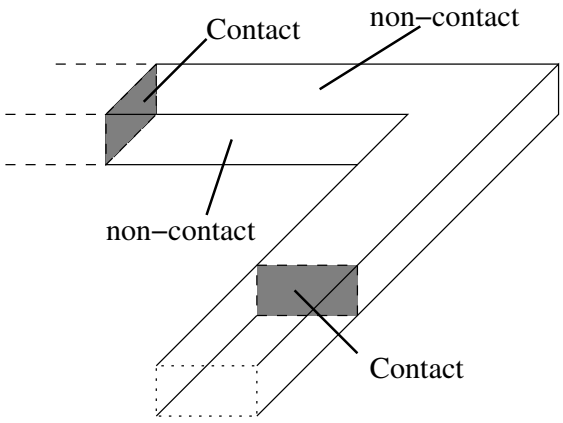

Figure 1: The surface of a 3D interconnect conductor

Subtract (14) from (13), we obtain

$$\begin{aligned} -\frac{1}{2}\vec{E}(\vec{r}) &= \nabla\phi(\vec{r})-\nabla\times\int_S dS(\vec{r}')G_0(\vec{r},\vec{r}')[\hat{n}\times\vec{E}](\vec{r}') \\ &+\nabla\int_S dS(\vec{r}')G_0(\vec{r},\vec{r}')[\hat{n}\cdot\vec{E}](\vec{r}') \\ &-(j\omega\mu_0)\int_S dS(\vec{r}')G_0(\vec{r},\vec{r}')[\hat{n}\times\vec{H}](\vec{r}'),\ \vec{r}\in S. \end{aligned} \tag{16}$$

Equations (8), (15) and (16) are the main integral equations in our formulation. Similar to the surface formulation in FastImp, using MPIE not only eliminates the volume integral term but also takes into account the coupling among conductors. In addition, the introduction of scalar potential ϕ into our formulation makes it very convenient to add voltage excitation into our system, just like PEEC models [19].

2.3 Boundary Conditions

The surface of each conductor could be divided into two non-overlapping parts: contact surfaces and non-contact surfaces, as shown in figure 1. The contact is an artificially exposed surface. It is created primarily to separate a block of 3-D interconnect from other parts within a large chip. Eventually a contact will correspond to a terminal in an equivalent circuit model. Since we choose to use voltage as the excitation to our system, the boundary condition on a contact is

$$\phi(\vec{r}) \equiv \phi_{e,i},\ \vec{r}\in S_{c,i} \tag{17}$$

where $S_{c,i}$ denotes the contact part of the i-th conductor surface and $\phi_{e,i}$ is the excitation potential on the i-th conductor.

Since the conductors connected to contacts are generally not included into the computational domain, we actually do not have any information about the material property of these conductors. It is because of this reason that we want to avoid using matching boundary conditions on the conductor surfaces in our formulation.

Non-contact surfaces are the portion of surfaces actually exposed to the surrounding medium. So we expect to see charge accumulating on the surfaces. In view of (3) and (4), this suggests that the boundary condition on the non-contact surfaces should be

$$\hat{n}(\vec{r})\cdot\vec{E}(\vec{r}) = \frac{j\omega\rho(\vec{r})}{\sigma_i},\ \vec{r}\in S_{nc,i}, \tag{18}$$

where $S_{nc,i}$ is the non-contact part of the i-th conductor surface.

2.4 Complete Formulation

Proceedings of the International Conference on Computer Aided Design (ICCAD'03)
1092-3152/03 $ 17.00 © 2003 ACM

From basic vector identity, we have

$$\begin{aligned}\nabla_s \cdot [\hat{n} \times \vec{H}] &= \nabla \cdot [\hat{n} \times \vec{H}] \\ &= \vec{H} \cdot \nabla \times \hat{n} - \hat{n} \cdot \nabla \times \vec{H}\end{aligned} \tag{19}$$

$$\begin{aligned}\nabla_s \cdot [\hat{n} \times \vec{E}] &= \nabla \cdot [\hat{n} \times \vec{E}] \\ &= \vec{E} \cdot \nabla \times \hat{n} - \hat{n} \cdot \nabla \times \vec{E},\end{aligned} \tag{20}$$

where $\nabla_s = \nabla - \hat{n}\frac{\partial}{\partial n}$. Since we are only considering flat conductor surfaces in this paper, $\hat{n}$ can be considered a constant vector. Then using (1) and (2), equations (19) and (20) can be simplified to

$$\nabla_s \cdot [\hat{n} \times \vec{H}](\vec{r}) = -(j\omega\varepsilon_0 + \sigma_i)E_n(\vec{r}),\ \vec{r} \in S_i \tag{21}$$

$$\nabla_s \cdot [\hat{n} \times \vec{E}](\vec{r}) = (j\omega\mu_0)H_n(\vec{r}),\ \vec{r} \in S_i. \tag{22}$$

Substituting (21) in (16) and (18) and (22) in (8) eliminates H_n in (8) and E_n in (16) and (18).

With all the boundary conditions and the simplified surface integral representations, the proposed surface integral formulation is summarized as the following:

$$\begin{aligned}&-\frac{1}{2}[\hat{n} \times \vec{E}](\vec{r}) = \hat{n}(\vec{r}) \times \nabla\phi(\vec{r}) - \hat{n}(\vec{r}) \times \nabla \times \int_S dS(\vec{r}')G_0(\vec{r},\vec{r}')[\hat{n} \times \vec{E}](\vec{r}') \\ &+\hat{n}(\vec{r}) \times \nabla \int_S dS(\vec{r}')G_0(\vec{r},\vec{r}')\frac{\nabla_s \cdot [\hat{n} \times \vec{H}](\vec{r}')}{(j\omega\varepsilon_0 + \sigma)} \\ &-(j\omega\mu_0)\hat{n}(\vec{r}) \times \int_S dS(\vec{r}')G_0(\vec{r},\vec{r}')[\hat{n} \times \vec{H}](\vec{r}'),\ \vec{r} \in S\end{aligned} \tag{23}$$

$$\begin{aligned}&\frac{1}{2}[\hat{n} \times \vec{H}](\vec{r}) = -\hat{n}(\vec{r}) \times \nabla \times \int_{S_i} dS(\vec{r}')G_1(\vec{r},\vec{r}')[\hat{n} \times \vec{H}](\vec{r}') \\ &+\hat{n}(\vec{r}) \times \nabla \int_{S_i} dS(\vec{r}')G_1(\vec{r},\vec{r}')\frac{\nabla_s \cdot [\hat{n} \times \vec{E}](\vec{r}')}{j\omega\mu_0} \\ &-(j\omega\varepsilon_0 + \sigma_i)\hat{n}(\vec{r}) \times \int_{S_i} dS(\vec{r}')G_1(\vec{r},\vec{r}')[\hat{n} \times \vec{E}](\vec{r}'),\ \vec{r} \in S_i\end{aligned} \tag{24}$$

$$\phi(\vec{r}) = \int_S dS(\vec{r}')G_0(\vec{r},\vec{r}')\frac{\rho(\vec{r}')}{\varepsilon_0},\ \vec{r} \in S \tag{25}$$

$$\nabla_s \cdot [\hat{n} \times \vec{H}](\vec{r}) = \frac{-j\omega(j\omega\varepsilon_0 + \sigma_i)\rho(\vec{r})}{\sigma_i},\ \vec{r} \in S_{nc,i} \tag{26}$$

$$\phi(\vec{r}) \equiv \phi_{e,i},\ \vec{r} \in S_{c,i}. \tag{27}$$

Equations (24) and (23) are obtained by restricting $\vec{r}$ on the inner side of the conductor surfaces and then keeping only the tangential components of (8) and (16). Since the two equations (21) and (22) are the normal components of the two fundamental equations (1) and (2), it would be redundant to enforce the normal component of the integral equations (8) and (16). This formulation has six scalar unknowns: two tangential components of $\vec{E}$ and $\vec{H}$, and two scalars ϕ and ρ. Equation (26) and (27) complement each other, so the total number of scalar equations is also six.

The two tangential components $\hat{n} \times \vec{E}$ and $\hat{n} \times \vec{H}$ are approximated with RWG basis functions, the edge-based linear basis function [20]. This generally requires that the conductor surfaces should be discretized with triangular panels. The two scalar variables ρ and ϕ are approximated with piecewise constant basis functions. The Galerkin scheme is used to test equations (24) and (23), and the collocation method is used to test (25).

If the electro-magneto-quasi-static (EMQS) approximation is assumed, the wave number k_0 in (12) can be simplified as $k_0 = 0$. If the magneto-quasi-static (MQS) approximation is assumed, then in addition to use $k_0 = 0$, the charge density ρ is zero in equation (26) and equation (25) is eliminated.

3. Advantages of the New Formulation

3.1 Use Dyadic Multilayered Green's Functions

As is shown in [21], this new surface formulation can make use of the dyadic multilayered media Green's functions [12, 15], primarily because the equations are derived using the vector Helmholtz wave equation. The surface integral formulation in FastImp, however, is derived from the scalar Helmholtz equation and to the best of the authors knowledge, multilayered Green's functions have not been derived for that case.

3.2 Consistent Port Current Calculation Method

One straight-forward way to calculate current on a contact S_c is

$$I = \int_{S_c} dS(\vec{r}')\sigma E_n. \tag{28}$$

As frequency increases, and skin effects cause current to crowd near the corners, it is necessary to discretize more finely so as to capture the exponential decay of the current density. Instead, a different scheme can be used once the frequency surpasses a point where the skin-depth is comparable to the cross-section size of the conductors. For the high frequency case, the current is calculated from

$$\begin{aligned}I &= \frac{\sigma}{\sigma + j\omega\varepsilon_0}\int_{S_c} dS(\vec{r}')\nabla \times \vec{H} \cdot \vec{n} \\ &= \frac{-\sigma}{(\sigma + j\omega\varepsilon_0)(j\omega\mu_0)}\int_L dl\nabla \times \vec{E} \cdot \hat{t}_l \\ &= \frac{-\sigma}{(\sigma + j\omega\varepsilon_0)(j\omega\mu_0)}\int_L dl(\frac{\partial E_n}{\partial t_f} - \hat{t}_f \cdot \frac{\partial \vec{E}}{\partial n}),\end{aligned} \tag{29}$$

where two tangential unit vectors $\hat{t}_l$ and $\hat{t}_f$ along with the normal unit vector $\hat{n}$ are in the local coordinate system.

Since the formula in (28) is inaccurate at high frequencies, and the formula in (29) is inaccurate at low frequencies, it is a relatively simple matter to switch between port current formulas depending on excitation frequency [6, 11]. However, such an approach can introduce discontinuties or interfere with model order reduction. The problem of switching formulas can be avoided in our new formulation.

The surface formulation in [6, 11] does not use the magnetic field as one of its variables. In our new formulation, however, we have $\hat{n} \times \vec{H}$ as a variable, so its accuracy is guaranteed by the solver we use for the discretized system. Using the magnetic field, the current can be calculated simply by

$$I = \sigma\int_{S_c} dS(\vec{r}')E_n = \frac{\sigma}{\sigma + j\omega\varepsilon_0}\int_{S_c} dS(\vec{r}')\nabla_s \cdot (\hat{n} \times \vec{H}(\vec{r}')) \tag{30}$$

Therefore, accuracy in $\hat{n} \times \vec{H}$ directly translates into accuracy in the current.

3.3 Apply RWG and Loop-Star Basis Functions

As pointed out in [22], direct application of the conventional RWG basis in the Electric Field Integral Equations (EFIE) formulation [23] results in a low frequency accuracy problem. Since the first two equations in our formulation are very similar to EFIE, the formulation also has this low-frequency problem. The key observation in [22] is that $\vec{E}$ field and $\vec{H}$ field have a divergence-free and a curl-free part that scale very differently with frequency. This leads to large numerical error when one part dominates. The loop-star basis function naturally decomposes the fields into the two parts, the loop basis approximates the divergence-free part and star basis approximates the curl-free part, so that each part can be

Proceedings of the International Conference on Computer Aided Design (ICCAD'03)
1092-3152/03 $ 17.00 © 2003 ACM

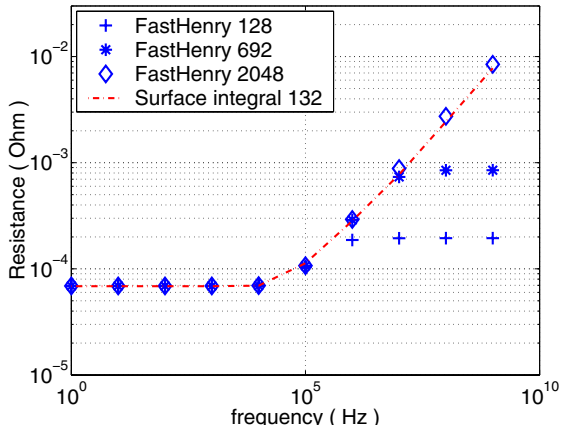

Figure 2: Resistance of a straight wire

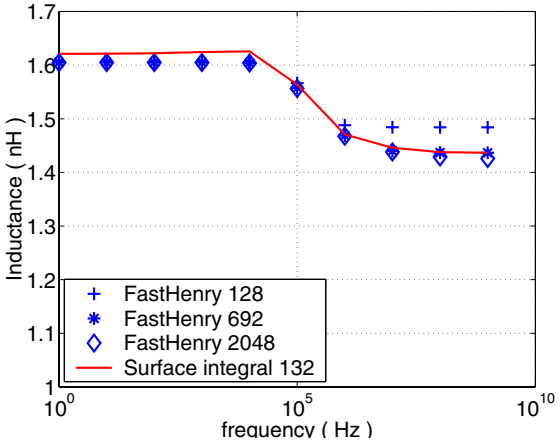

Figure 3: Inductance of a straight wire

scaled separately [24, 25]. Although the derivation is lengthy, it is possible to show that the new formulation can be used in conjunction with loop-star basis functions [21].

4. Numerical Results

In this section we present some computational results using the new surface formulation. The formulation was implemented using Matlab, and the implementation includes the loop-star basis and frequency normalization. To test the formulation, we used simple wire and ring structures to compare results from the MQS analysis program FastHenry to results generated using our implementation of the new formulation simplified to perform MQS analysis. The numerical experiments demonstrate that the new surface integral formulation is accurate and robust across a wide frequency range. The numerical experiments also show we can indeed accurately compute port current at both low and high frequencies with the single method in (30).

4.1 A straight wire

For the wire example, we used a wire with a cross-section of 1*mm* by 1*mm*, a length was 4*mm*, and the conductivity of copper, 5.8*e*7. The conductor surface was discretized into 132 triangular panels, and both our new formulation and FastHenry were used to calculate the wire resistance and inductance. The comparison with FastHenry is shown in figure 2 and 3. Note that the number of filaments used with FastHenry was increased from 128, to 692, and finally to 2048 to demonstrate the need for fine discretization to capture skin effects. The plots clearly show that our new formulation uses a single discretization yet is accurate across a wide frequency range.

4.2 A ring

For the ring example, we used a ring with a 10*mm* radius, a 0.5*mm* by 0.5*mm* square cross section, and a conductivity 5.8e7 (copper). The conductor surface was discretized into 272 triangular panels, and both our new formulation and FastHenry were used to calculate the wire resistance and inductance. Note that the number of filaments used with FastHenry was increased from 960, to 3840, and finally to 15360 to demonstrate the need for fine discretization to capture skin effects. Note also that at low frequency, the relative error of both resistance and inductance is about 5 percent. This error is primarily due to the 272 panel discretization's inability to accurately represent the geometry, as there are only 16 panels along the circular direction of ring. Finally, the error is larger at high frequencies mainly because the coarse discretization of the surface is insufficient to capture crowding of current near corners at high frequencies. Clearly, even the surface formulation requires some discretization adjustments to handle high frequencies.

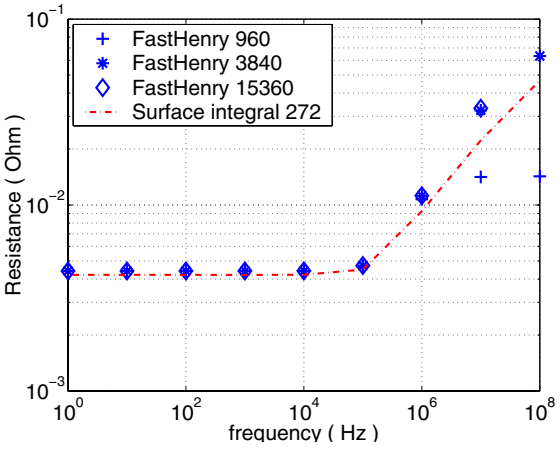

Figure 4: Resistance of a ring

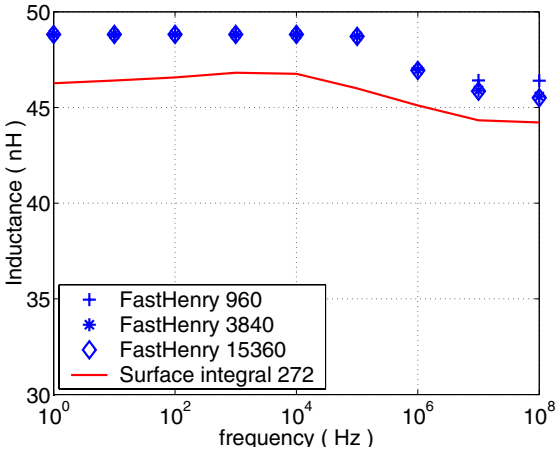

Figure 5: Inductance of a ring

Proceedings of the International Conference on Computer Aided Design (ICCAD'03)
1092-3152/03 $ 17.00 © 2003 ACM

5. Conclusions

We have proposed a new surface integral formulation for the Magneto-Quasi-Static, Electro-Magneto-Quasi-Static and fullwave analysis of complicated 3D structures embedded in multilayered media. This formulation is closely linked with the well-known Stratton-Chu formulation or EFIE and MFIE formulation. Hence the well-established techniques like RWG linear basis function, loop-star basis transformation and frequency normalization can be used to reduce the number of unknowns and to improve the accuracy at low frequencies. Numerical experiments show that the formulation is accurate and robust across wide frequency range.

The main advantages of this new formulation are its capability to handle multilayered Green's function and its compatibility with the standard model order reduction techniques. Since the prototype implementation was written in matlab, we have not presented CPU times. In addition, the code can only handle structures discretized into no more than a few hundred triangles. Our future work will be to combine this new integral formulation with: acceleration techniques to improve the efficiency, and model reduction to extract circuit models.

6. References

[1] K. Nabors and J. White, "FASTCAP: A multipole-accelerated 3-D capacitance extraction program," *IEEE Trans. on Computer-Aided Design*, vol. 10, pp. 1447–1459, November 1991.

[2] M. Kamon, M. J. Tsuk, and J. White, "Fasthenry: A multipole-accelerated 3-D inductance extraction program," *IEEE Transactions on Microwave Theory and Techniques*, vol. 42, no. 9, pp. 1750–1758, September 1994.

[3] J. R. Phillips and J. K. White, "A precorrected-FFT method for electrostatic analysis of complicated 3D structures," *IEEE Trans. Computer-Aided Design*, pp. 1059–1072, 1997.

[4] S. Kapur and J. Zhao, "A fast method of moments solver for efficient parameter extraction of mcms," 34^{th} *ACM/IEEE Design Automation Conference*, pp. 141–146, 1997.

[5] D. Luca, A. S. Vincentelli, and J. K. White, "Using conduction modes basis functions for efficient electromagnetic analysis of on-chip and off-chip interconnect," 38^{th} *ACM/IEEE Design Automation Conference*, 2001.

[6] J. Wang and J. K. White, "A wide frequency range surface integral formualtion for 3d rlc extraction," *International Conference on Computer Aided-Design*, 1999.

[7] K. M. Coperich, A. C. Cangellaris, and A. E. Ruehli, "Enhance skin effect for partial-element-equaivalent-circuit (peec) models," *IEEE Transactions on Microwave Theory and Techniques*, pp. 1435–1442, 2000.

[8] E. Tuncer, B.T. Lee, and D.P. Neikirk, "Interconnect series impedance determination using a surface ribbon method," 3^{rd} *IEEE Topical Meetings on Electrical Performance of Electronic Packaging*, pp. 249–252, November 1994.

[9] Z.H. Zhu, J. Huang, B. Song, and J. K. White, "Improving the robustness of a surface integral formulation for wideband impedance extractio of 3d structures," *International Conference on Computer Aided-Design*, 2001.

[10] Zhenhai Zhu, *Efficient Techniques for Wideband Impedance Extraction of Complex 3-D Geometries*, Master thesis MIT EECS Department, 2002.

[11] Z.H. Zhu, B. Song, and J. K. White, "Algorithms in fastimp: A fast and wideband impedance extraction program for complicated 3-d geometries," 40^{th} *ACM/IEEE Design Automation Conference*, 2003. Source code available for free download at rleweb.mit.edu/vlsi/codes.htm.

[12] K.A. Michalski and J.R. Mosig, "Multilayered media Green's functions in integral equation formulations," *IEEE Transactions on Antennas and Propagation*, vol. 45, pp. 508–519, March 1997.

[13] M.I. Aksun, "A robust approach for the derivation of closed-form Green's unctions," *IEEE Transactions on Microwave Theory and Techniques*, vol. 44, pp. 651–657, May 1996.

[14] E.J. Grimme, *Krylov projection methods for model order reduction*, PH.D. thesis UIUC EECS Department, 1997.

[15] C. T. Tai, *Dyadic Green's functions in electromagnetic theory*, IEEE Press, Piscataway, New Jersey, 1994.

[16] S. Ramo, J.R. Whinnery, and T.V. Duzer, *Fields and waves in communication electronics*, John Willey and sons, Inc., New York, 1994.

[17] J.A. Stratton, *Electromagnetic Theory*, McGraw-Hill Book Company, New York, 1941.

[18] R. F. Harrington, *Field Computation by Moment Methods*, MacMillan, New York, 1968.

[19] H. Heeb and A. E. Ruehli, "Three-dimensional interconnect analysis using partial element equivalent circuits," *IEEE Transactions on Circuits and Systems I:Fundamental Theory and Applications*, vol. 39, no. 11, pp. 974–982, November 1992.

[20] S.M. Rao, D.R. Wilton, and A.W. Glisson, "Electromagnetic scattering by surfaces of arbitrary shapes," *IEEE Transactions on Antennas and Propagation*, vol. 30, pp. 409–418, May 1982.

[21] Z.H. Zhu, B. Song, J.Rockway, and J. K. White, "A Stratton-Chu style surface integral formulation for impedance extraction of 3-d interconnect," *paper in preparation*.

[22] J.R. Mautz and R.F. Harrington, "An E-field solution for a conducting surface small or comparable to the wavelength," *IEEE Transactions on Antennas and Propagation*, vol. 32, pp. 330–339, April 1984.

[23] W.C. Chew, *Waves and fields in inhomogeneous media*, IEEE Press, New Jersey, 1995.

[24] G. Vecchi, "Loop-star decomposition of basis functions in the discretization of the efie," *IEEE Transactions on Antennas and Propagation*, vol. 47, pp. 339–346, February 1999.

[25] J.S. Zhao and W.C. Chew, "Integral equation solution of maxwell equations from zero frequency to microwave frequencies," *IEEE Transactions on Antennas and Propagation*, vol. 48, pp. 1635–1645, October 2000.

Proceedings of the International Conference on Computer Aided Design (ICCAD'03)
1092-3152/03 $ 17.00 © 2003 ACM